Estimating Mixed Layer Depth from Oceanic Profile Data

RICHARD E. THOMSON

Institute of Ocean Sciences, Sidney, British Columbia, Canada

ISAAC V. FINE

Institute of Ocean Sciences, Sidney, British Columbia, Canada, and Heat and Mass Transfer Institute, National Academy of Sciences, Minsk, Belarus

(Manuscript received 29 December 2001, in final form 7 August 2002)

ABSTRACT

Estimates of mixed layer depth are important to a wide variety of oceanic investigations including upper-ocean productivity, air–sea exchange processes, and long-term climate change. In the absence of direct turbulent dissipation measurements, mixed layer depth is commonly derived from oceanic profile data using threshold, integral, least squares regression, or other proxy variables. The different methodologies often yield different values for mixed layer depth. In this paper, a new method—the split-and-merge (SM) method—is introduced for determining the depth of the surface mixed layer and associated upper-ocean structure from digital conductivity–temperature–depth (CTD) profiles. Two decades of CTD observations for the continental margin of British Columbia are used to validate the SM method and to examine differences in mixed layer depth estimates for the various computational techniques. On a profile-by-profile basis, close agreement is found between the SM and de facto standard threshold methods. However, depth estimates from these two methods can differ significantly from those obtained using the integral and least squares regression methods. The SM and threshold methods are found to approximate the ''true'' mixed layer depth whereas the integral and regression methods typically compute the depth of the underlying pycnocline. On a statistical basis, the marginally smaller standard errors for spatially averaged mixed layer depths for the SM method suggest a slight improvement in depth determination over threshold methods. This improvement, combined with the added ability of the SM method to delineate simultaneously ancillary features of the upper ocean (such as the depth and gradient of the permanent pycnocline), make it a valuable computational tool for characterizing the structure of the upper ocean.

1. Introduction

Turbulence generated in the ocean by the wind, convective cooling, breaking waves, current shear, and other physical processes creates a surface layer characterized by uniform to near-uniform density, active vertical mixing, and high dissipation (e.g., Wijesekera and Gregg 1996). The depth of this ''mixing layer'' (Brainerd and Gregg 1995) is ultimately determined by a balance between the destabilizing effects of mechanical mixing and the stabilizing effects of surface buoyancy flux. Because of temporal variations in turbulence intensity and buoyancy flux, the mixing layer may be embedded in a deeper ''mixed layer'' of almost identical density to the mixing layer and representing the time-integrated response to previous mixing events. Mixed layer depth can vary by tens of meters over a diurnal cycle (Price et al. 1986; Denman and Gargett 1988; Schneider and Müller 1990) and by 100 m over an annual cycle (Dodimead et al. 1963; Sprintall and Roemmich 1999).

Numerous studies have emphasized the importance of mixed layer depth (MLD) estimation to upper-ocean processes and variability (cf. Curry and Roy 1989; Robinson et al. 1993; Wijesekera and Gregg 1996; Kara et al. 2000a,b). Much of our physical understanding of MLDs stems from an interest in transient, short-term ($<$1 day) fluctuations in sea surface temperature and the accompanying exchanges of heat, carbon dioxide, and other properties with the overlying atmosphere [cf. the review by Large et al. (1994) and numerical modeling work by Garwood (1977), Martin (1985), and Kantha and Clayson (1994)]. In these studies, the mixed layer—referred to as the diurnal mixed layer (DML) by Smyth et al. (1996a,b)—is defined as the uppermost layer of uniform density, high turbulent dissipation, and diurnal restratification. The commonly used threshold difference method (cf. Table 1) defines the base of the mixed layer as the depth at which the potential density, σ_θ, in the upper layer changes by 0.01 kg m^{-3} relative to the ocean surface density. Although this definition is probably too narrow for biological applications—it often

Corresponding author address: Dr. Richard E. Thomson, Institute of Ocean Sciences, P.O. Box 6000, 9860 West Saanich Rd., Sidney, BC V8L 4B2, Canada.
E-mail: thomsonr@pac.dfo-mpo.gc.ca

TABLE 1. Selected definitions for mixed layer depth and other upper-ocean features. Here, T is temperature, S is salinity, and σ_θ is potential density. The ''trapping depth,'' D_T (Price et al. 1986), is analogous to the integral depth scale [Eq. (2.4)].

Source	Name	Definition
Price et al. (1986)	Trapping depth, D_T	$D_T = \Delta T^{-1} \int_{z_i}^{z} T\, dz$
Peters et al. (1989)	Mixed layer depth, MLD	$\Delta\sigma_\theta = 0.01$ kg m^{-3} (relative to $z = 0$ m)
Schneider and Müller (1990)	Mixed layer depth, MLD	$\Delta\sigma_\theta = 0.01$ kg m^{-3} (relative to $z = 2.5$ m); $\Delta\sigma_\theta = 0.03$ kg m^{-3} (relative to $z = 2.5$ m)
Wijffels et al. (1994)	Mixed layer depth, MLD; top of thermocline, TTC	$\Delta\sigma_\theta = 0.01$ kg m^{-3} (relative to $z = 2.5$ m); $\partial\sigma_\theta/\partial z = 0.01$ kg m^{-4}
Brainerd and Gregg (1995)	Mixed layer depth, MLD	$\Delta\sigma_\theta = 0.005$–$0.5$ kg m^{-3}; $\partial\sigma_\theta/\partial z = 0.0005$–$0.05$ kg m^{-4}
Smyth et al. (1996a,b)	Diurnal mixed layer, DML; upper-ocean layer, UOL	$\Delta\sigma_\theta = 0.01$ kg m^{-3}; $\sigma_\theta < 22$ kg m^{-3} (top of pycnocline)
Weller and Plueddemann (1996)	Mixed layer depth, MLD; isopycnal layer depth, ILD; seasonal thermocline depth, STD	$\Delta T = 0.01$°C (relative to $z = 2.25$ m); $\Delta\sigma_\theta = 0.03$ kg m^{-3} (relative to $z = 10$ m); $\Delta\sigma_\theta = 0.15$ kg m^{-3} (relative to $z = 10$ m)
Wijesekera and Gregg (1996)	MLD MLD_1 MLD_2 MLD_3	$\Delta\sigma_\theta = 0.01$ kg m^{-3} (relative to $z = 0$ m); $\partial\sigma_\theta/\partial z = 0.01$ kg m^{-4}; $\partial\sigma_\theta/\partial z = 0.025$ kg m^{-4}; $\partial S/\partial z = 0.01$ psu m^{-1}
Skyllingstad et al. (1999)	MLD	$\Delta\sigma_\theta = 0.01$ kg m^{-3} (relative to $z = 0$ m)

neglects the underlying water of near-identical density encompassing high chlorophyll, nutrient, and particle concentrations (e.g., Robinson et al. 1993; Washburn et al. 1998) and ignores the fact that ''the retreat of turbulent mixing to shallower depths proceeds faster than the erosion of the stratification at the base . . .'' (Kara et al. 2000a)—the threshold difference method with the specific threshold of 0.01 kg m^{-3} has emerged as the de facto standard by which different methods and studies are compared.

Methods for estimating the MLD from profile data fall into three broad categories (cf. Schneider and Müller 1990; also, Table 1): 1) threshold methods, which find a predefined step in the surface profile (Price et al. 1986; Lukas and Lindstrom 1991; Peters et al. 1988) or a critical gradient for the upper layer (Lukas and Lindstrom 1991); 2) least squares regression methods, which fit two or more line segments to near-surface profiles (Papadakis 1981, 1985); and 3) integral methods, which calculate a depth scale for the upper layer (Freeland et al. 1997). Due to a lack of salinity data, or because salinity data tend to be noisier than temperature data, the MLD is sometimes linked to a steplike change in water temperature, with specified steps in the range 0.01°–0.5°C (e.g., Levitus 1982; Weller and Plueddemann 1996; Kara et al. 2000a,b). Where possible, it is preferable to use potential density or sigma t (σ_t) as estimators for MLD, primarily because it is the density structure that directly affects the stability and degree of turbulent mixing in the water column. In situ density is less reliable because overturning turbulence can result in adiabatic changes of 0.04 kg m^{-3} over depths of 10 m (Schneider and Müller 1990).

This paper has a twofold purpose: 1) to introduce a split-and-merge (SM) algorithm for estimating the depths of the surface mixed layer and underlying features from oceanic profile data and 2) to compare results for the different estimators of mixed layer depth presently in use based on several decades of profile data collected off the west coast of Canada. Formulation of the SM method originated from our need for a realistic annual cycle in mixed layer depth for ecosystem models being developed for the west coast of Vancouver Island, British Columbia (Robinson et al. 1993; Robinson and Ware 1994). A report on these models (C. Robinson 1997, personal communication) concluded that, ''In general, the upwelling rate and the minimum depth of the summer mixed layer depth (off southwest Vancouver Island) result in the greatest variability in annual plankton or fish production.'' For our purpose, we found existing techniques for estimating mixed layer depth either too tightly constrained (e.g., the standard threshold method) or too loosely defined (e.g., the integral depth-scale method). The SM method is shown to be a computationally efficient and flexible curve-fitting technique that combines accurate estimation of mixed layer depth with the versatility to define other upper-ocean features, such as the depth of the top of the thermocline and the gradient of the main pycnocline.

2. Conventional methods

A common approach for estimating the surface mixed layer depth is to specify a threshold slope for the vertical density gradient (e.g., Price et al. 1986; Lukas and Lindstrom 1991) or a threshold for the density offset relative to the ocean surface (e.g., Peters et al. 1989; Schneider and Müller 1990; Wijffels et al. 1994; Weller and Plueddemann 1996). The density gradient method is considered a less consistent estimator of MLD than the density difference approach (Schneider and Müller 1990). Because of the eddylike scales of turbulent mechanical mixing, density profiles are often piecewise-linear rather than smoothing varying. As a consequence, MLD also can be equated to the uppermost line segment in least squares approximations to steplike density profiles (Papadakis 1981; Freeland et al. 1997) or to the integral depth scale for the surface layer (Price et al. 1986; Freeland et al. 1997). Papadakis (1981, 1985) used a three-line approximation to estimate the MLD in terms of abrupt changes (''break points'') in the profiles.

a. Threshold method

In air–sea interaction studies (e.g., Wijesekera and Gregg 1996; Smyth et al. 1996a,b), the depth of the surface mixed layer is defined as that depth z at which the potential density difference $\Delta\sigma_\theta(z) = \sigma_\theta(z) - \sigma_\theta(z_0)$ in the upper ocean exceeds a specified threshold value, commonly 0.01 kg m^{-3} (Fig. 1a); here z_0 is a reference depth (generally in the range $z_0 = 0$, the ocean surface, to 10 m), and $\sigma_\theta(z) = \rho_\theta(z) - 1000$ kg m^{-3} is the density anomaly for measured potential density, ρ_θ. [For the less-used threshold gradient method, mixed layer depth is the depth at which the density gradient $\partial\sigma_\theta/\partial z$ first exceeds 0.01 kg m^{-4} (cf. Fig. 1b) or other specified level.] Because the threshold method is comparatively simple—depth estimates can be made by hand without analytical computations—and because the threshold difference of 0.01 kg m^{-3} generally yields diurnal depth estimates similar to those from turbulent dissipation measurements, the threshold difference method with the threshold 0.01 kg m^{-3} has become the de facto standard for many mixed layer depth studies. However, in ocean-climate studies, where the focus is on the variability in MLD averaged over periods of months and longer, threshold values in excess of 0.125 kg m^{-3} are more commonly used for monthly mean data (cf. Table 1 in Kara et al. 2000a).

b. Step-function least squares regression method

Problems with profile approximations have led to the formulation of customized curve-fitting algorithms for oceanic profiles, including the use of least squares linear approximations (Papadakis 1981; Freeland et al. 1997) and ''form oscillators'' (Papadakis 1985). Papadakis (1981) used a three-segment linear fit and the Newtonian approximation method to find a minimum variance solution to the general mixed layer depth problem; Freeland et al. (1997) used a two-segment least squares approach to obtain a time series of winter mixed layer depth at Ocean Weather Station P (50°N, 145°W) in the northeast Pacific. The two-segment case (Fig. 1c) can be solved analytically and is useful for pre-CTD data. The three-segment case requires special techniques (e.g., Papadakis 1985) and solutions can be unstable.

The two-segment approach seeks a least squares approximation to a steplike water density, $f(z)$, such that

$$f(z) = \begin{cases} \sigma_{\theta 1} & z_a < z < D \\ \sigma_{\theta 2} & D < z < z_b, \end{cases} \tag{2.1}$$

where z_a is a near-surface depth; D is the estimated mixed layer depth; z_b = 200–500 m is an arbitrary depth below the depth of seasonal mixing; and $\sigma_{\theta 1}$, $\sigma_{\theta 2}$ are constant potential densities for the mixed layer and intermediate layer, respectively. Minimizing the integral

$$\Phi = \int_{z_a}^{D} [\sigma_\theta(z) - \sigma_{\theta 1}]^2 \, dz + \int_{D}^{z_b} [\sigma_\theta(z) - \sigma_{\theta 2}]^2 \, dz \tag{2.2}$$

leads to three equations for $\sigma_{\theta 1}$, $\sigma_{\theta 2}$, and D with the solution

$$F(D) = \sigma_\theta(D) - \frac{1}{2}\left[\frac{\int_{z_a}^{D} \sigma_\theta(z)\, dz}{D - z_a} + \frac{\int_{D}^{z_b} \sigma_\theta(z)\, dz}{z_b - D}\right] = 0, \tag{2.3}$$

which can be solved numerically. Two-segment approximations are computationally stable. Increasing the number of segments or ''steps'' can improve the approximation to the profile data but typically leads to greater complexity. The quality of the least squares fit varies from profile to profile depending on the structure of the underlying layering.

c. Integral depth-scale method

A simple estimate of the mixed layer depth is the integral depth scale (Fig. 1d) [also called the trapping depth by Price et al. (1986)]:

$$D = \frac{\int_0^{z_b} zN_b^2(z)\, dz}{\int_0^{z_b} N_b^2(z)\, dz} = \frac{\int_{z_a}^{z_b} (\sigma_{\theta b} - \sigma_\theta)\, dz}{\sigma_{\theta b} - \sigma_{\theta a}}, \tag{2.4}$$

where, as in the previous section, z_a and z_b are a near-

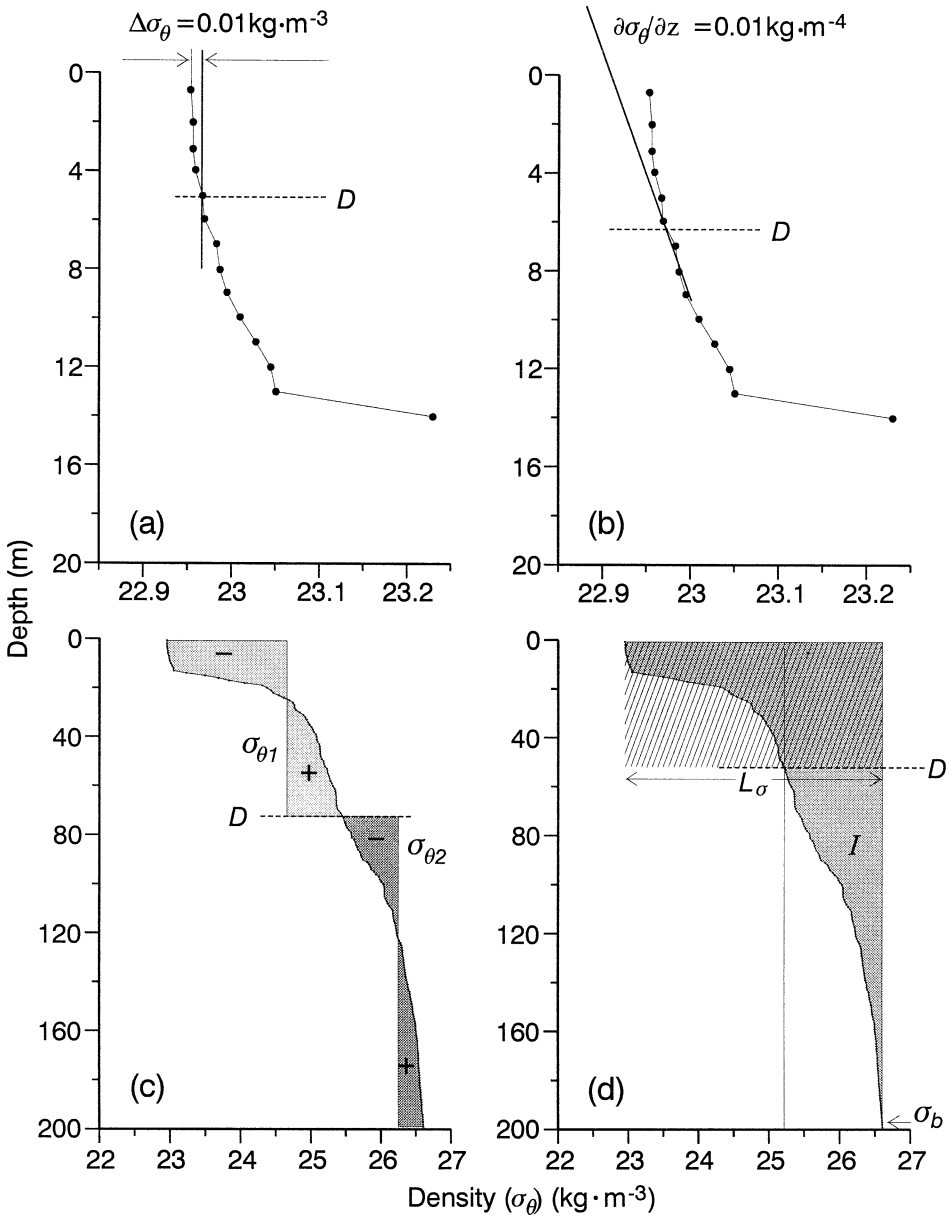

FIG. 1. Estimation of mixed layer depth (D) for different methods for the density profile obtained for station LH07 on the west coast of Vancouver Island on 19 Jul 1997 (see Fig. 3 for station location). (a) Threshold difference method with standard density step $\Delta\sigma_\theta(z) = \sigma_\theta(z) - \sigma_\theta(0) = 0.01$ kg m^{-3}; (b) threshold gradient method for $\partial\sigma_\theta/\partial_z = 0.01$ kg m^{-4}; (c) two-segment least squares method [cf. Eqs. (2.1)–(2.3)] for $z_a = 10$ m, $z_b = 200$ m, constant $\sigma_{\theta 1}$ and $\sigma_{\theta 2}$, and $\sigma(D) = (\sigma_{\theta 1} + \sigma_{\theta 2})/2$; and (d) integral depth scale, D, with $z_a = 10$ m and $z_b = 200$ m [Eq. (2.4)]. In (c), each of the paired shaded regions have equal positive (+) and negative (−) areas. In (d), the darkly shaded rectangle has sides of length D and $L_\sigma = \sigma_\theta(z_b) - \sigma_\theta(z_a)$, with the area $D \times L$ of the rectangle equal to the integral $I = \int_{z_b}^{z} [\sigma_\theta(z) - \sigma_{\theta b}]\, dz$ denoted by the shaded region to the right of the density profile.

surface depth and an arbitrary reference depth, and $\sigma_{\theta b} = \sigma_\theta(z_b)$, $\sigma_{\theta a} = \sigma_\theta(z_a)$ (cf. Freeland et al. 1997). Here,

$$N_b(z) = \left(-\frac{g}{\rho_0} \frac{d\rho_\theta}{dz} \right)^{1/2} \tag{2.5}$$

is the buoyancy (Brunt–Väisälä) frequency, g is the acceleration of gravity, and ρ_0 is a reference density. Unlike the threshold methods, which often require only the upper portion of a density profile, the step-function and integral-depth approaches require specification of a deep reference density that is generally much deeper than the mixed layer depth.

3. The split-and-merge algorithm

Application of the threshold difference method to the 4811 CTD profiles collected from Canadian Department

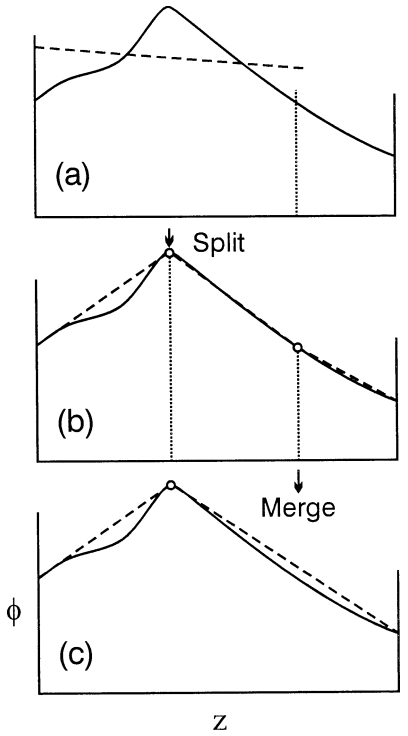

FIG. 2. Illustration of the SM algorithm applied to a case where the optimum segmentation can be found in single iterations (after Pavlidis and Horowitz 1974). The initial fit (dashed line) to the left-hand segment of the curve $\phi(z)$ is split at the break point to form three separate segments. The two right-hand segments are then merged to form one segment.

of Fisheries and Oceans research vessels working off the west coast of Vancouver Island from 1978 to 2000 yielded instances where the estimated mixed layer depth differed markedly from the visually estimated mixed layer depth (i.e., the depth to the top of the first pycnocline estimated from density plots). This, and our conclusion that depth estimates from the step-function and integral-scale methods were more representative of the main pycnocline depth rather than the surface mixed layer depth, caused us to seek a more reliable method for estimating mixed layer depth. Moreover, because the separation of profile data into distinct layers is of oceanographic importance, we wanted a method that could simultaneously approximate other upper-ocean structural features in addition to the mixed layer depth. For these applications, we turned to the SM algorithm developed by Pavlidis and Horowitz (1974) to estimate the optimal decomposition of plane curves and waveforms.

a. Methodology

The SM algorithm approximates a specified curve using piecewise polynomial functions (or other specified functions) in which the break points in the fitted curve—locations of subset boundaries such as changes in slope or steplike offsets—are adjusted to fit the available data (Fig. 2). The algorithm provides profile decomposition by defining the locations of the break points separating the different segments, together with the piecewise approximation parameters and the error of the approximation. In general, the fitted segments are disjointed but can be made to satisfy a continuity requirement by a retrospective local adjustment of the approximating curves. We consider the problem of fitting a series of segments to the profile, $\phi(z)$, where z is depth and ϕ represents temperature, salinity, density, fluorescence, or other profile variable. Given a set of points $S = \{z_i, \phi_i\}$, $i = 1, 2, \ldots, N$, we seek the minimum number n such that S is divided into n subsets $S_1, S_2, \ldots, S_n$ in which the data points for each subset are approximated by a polynomial of order at most $m - 1$ with an error norm that is less than some specified quantity ε. Here, ''error norm'' is the root-mean-square (rms) difference, maximum difference, or other statistical measure of the difference between the observed and fitted curves for a given subset (cf. the appendix). The SM algorithm merges adjacent fitted segments with similar approximating coefficients and splits those segments with unacceptable error norms. A least squares method, or similar approach, is used to fit the curve to the specified dataset. Because fitting higher-order polynomials has its own set of problems, we restrict our discussion to piecewise-linear approximations for which $m = 2$. The uppermost segment (representing the mixed layer) is assumed to have a near-uniform vertical distribution so that $m = 1$ for this segment.

The SM method removes the need for the careful a priori choice of the number of segments n as well as the need to specify the initial segmentation. In this way, it is straightforward to obtain segmentation where the error norm on each segment (or over all segments) does not exceed a specified bound. Computational time is of order N. For a specified error norm, we equate the mixed layer depth D with the uppermost (constant) segment of the piecewise-linear fit. (See the appendix for further details on the SM method.)

To avoid scaling problems for profile variables, including the need for a different error norm for each variable, we have normalized both z and ϕ (z) such that

$$z^* = \frac{z - z_{\min}}{z_{\max} - z_{\min}}; \qquad \phi^*(z) = \frac{\phi(z) - \phi_{\min}}{\phi_{\max} - \phi_{\min}}, \quad (3.1)$$

where subscripts denote the maximum and minimum values of the given variable over the depth range of interest and $0 \leq [z^*, \phi^*(z)] \leq 1$. Following other authors (see Table 1), we have used a nonzero starting depth (here, $z_{\min} = 2.5$ m), to avoid the effects of propwash and turbulent flow past the hull of the ship during station keeping, and $z_{\max} = 150$ m to ensure capture of the mixed layer depth regardless of season. As with the threshold method, the SM algorithm requires a predefined error norm ε. To determine the sensitivity of MLD

estimates to the specified error norm, we examined estimates over a wide range of ε values, from 0.001 to 0.03, and found that results for $\varepsilon = 0.01$ best corresponded to our ''visual'' MLD estimates. This error norm also coincides closely with accepted threshold values for the established threshold method, giving further support for the SM approach. We note that $\varepsilon = 0.01$ yields a mean MLD of 15.4 m, the same mean MLD obtained for the threshold $\Delta\sigma_\theta = 0.03$ kg m^{-3}. The smaller error norm $\varepsilon = 0.003$ yields a slightly smaller mean MLD of 12.4 m, which is similar to the mean MLD obtained from the ''standard'' threshold $\Delta\sigma_\theta = 0.01$ kg m^{-3}. We therefore use the error norm $\varepsilon = 0.003$ when making direct comparisons of the SM and standard threshold methods.

Figure 3 provides examples of SM estimates of mixed layer depth for CTD profiles collected in July 1997 along ship survey lines B, D, H, and M off the west coast of Vancouver Island (see insert in Fig. 3). In almost all cases, the depth estimates for the SM method with $\varepsilon = 0.01$ are consistent with our visual estimations of the mixed layer depth. Similar findings are obtained for different lines and different summer survey data.

b. Comparison of methods

All CTD profiles collected seaward of Vancouver Island from 1978 to 2000 have been used to compare results from the SM method with those from conventional methods. Figure 4a presents an example of a well-defined mixed layer in which the upper layer has uniform density and is underlaid by a sharp pycnocline. For this example, the threshold and SM methods give nearly identical MLD results over a wide range of threshold and error norm values. We note, however, that for the threshold method the MLD estimate increases with increased threshold while for the SM method, the MLD estimate remains unchanged over a wide range of norm values (i.e., is less sensitive to the choice of error). The underlying pycnocline is closely approximated by the SM method, demonstrating the method's considerable flexibility.

Figure 4b presents a more complicated case in which the upper layer has a weak density gradient. Here, the ability of the threshold method to estimate the MLD is strongly dependent on the threshold value. In contrast, the SM algorithm finds an MLD that corresponds closely to the visual estimate. When the upper layer has a ''significant'' density gradient (as in Fig. 4c), both the threshold and SM methods have difficulty estimating a mixed layer depth. In such cases, there is no well-defined mixed layer and depth estimates invariably depend on the specified error values. In particular, if the profile has a measurable pycnocline in the upper portion of the profile, the SM algorithm will find the start depth of the layer, which in our case has been set to 2.5 m (Fig. 4c). Similar results were found scattered throughout the 21-yr dataset.

Table 2a presents a statistical summary of the mean depths and standard deviations for all five methods for all density profiles collected off the west coast of Vancouver Island. Results for the threshold difference method (TH) are based on the threshold $\Delta\sigma_\theta = 0.01$ kg m^{-3} and those for the threshold gradient method (GR) on a gradient $\Delta\sigma_\theta/\Delta z = 0.006$ kg m^{-4}. The specified error norm $\varepsilon = 0.003$ for the SM method coincides with the threshold difference of 0.01 kg m^{-3}. As the tabulated results indicate, the mean mixed layer depths obtained using the threshold and SM methods are markedly different from those based on the regression and integral methods. Mean depths from the threshold and SM methods (MLD $\approx$ 12 m) are a factor of 5 smaller than those for the regression and integral methods (MLD $\approx$ 60 m), and most accurately match visual estimates of the uniform-density surface mixed layer. Estimates from the regression and integral methods are more representative of the permanent pycnocline depth than the surface mixed layer depth.

Because the mean MLD estimates determined by the threshold and SM methods are nearly identical, we use a second-order statistic (the standard error) as a measure of the relative ''performance'' or predictive skill of a given method. The relatively small standard error (=standard deviation divided by $\sqrt{(N-1)}$, where N is the number of estimates) in mixed layer depth for the threshold and SM methods (Table 2a) confirms the ability of these methods to closely track short-period changes in layer depth. In contrast, the regression and integral methods—which provide a weighted depth for the main pycnocline—appear to be more affected by large-amplitude internal tides whose vertical displacements are typically largest within the pycnocline. The three-layer (D_3) regression method performed better than the two-layer (D_2) regression method, but it too proved unsatisfactory when the depth profile below the surface mixed layer became structurally complicated. According to Table 2b (which also includes a three-step SM analysis using $n = 3$), the covariance between the two-step regression and integral methods is relatively high ($r^2 = 0.71$), whereas the covariance between these methods and other methods is low ($r^2 < 0.15$). For the threshold and SM methods, within-group correlation is highest between the threshold difference and SM methods ($r^2 = 0.90$) and lowest between the SM and threshold gradient methods ($r^2 = 0.76$). Thus, based on computed means, standard errors, and covariances, we conclude that only the threshold and SM methods provide consistently accurate estimates of mixed layer depth.

Because the error norm $\varepsilon = 0.003$ for the SM method was selected to provide MLD estimates that were compatible with depth estimates obtained using the standard threshold and threshold gradient methods, the mean depths for all methods (12.4 m for the SM method and 12.5 m for the threshold difference and threshold gradient methods) are essentially identical. However, the variance in the mixed layer depth estimates—which

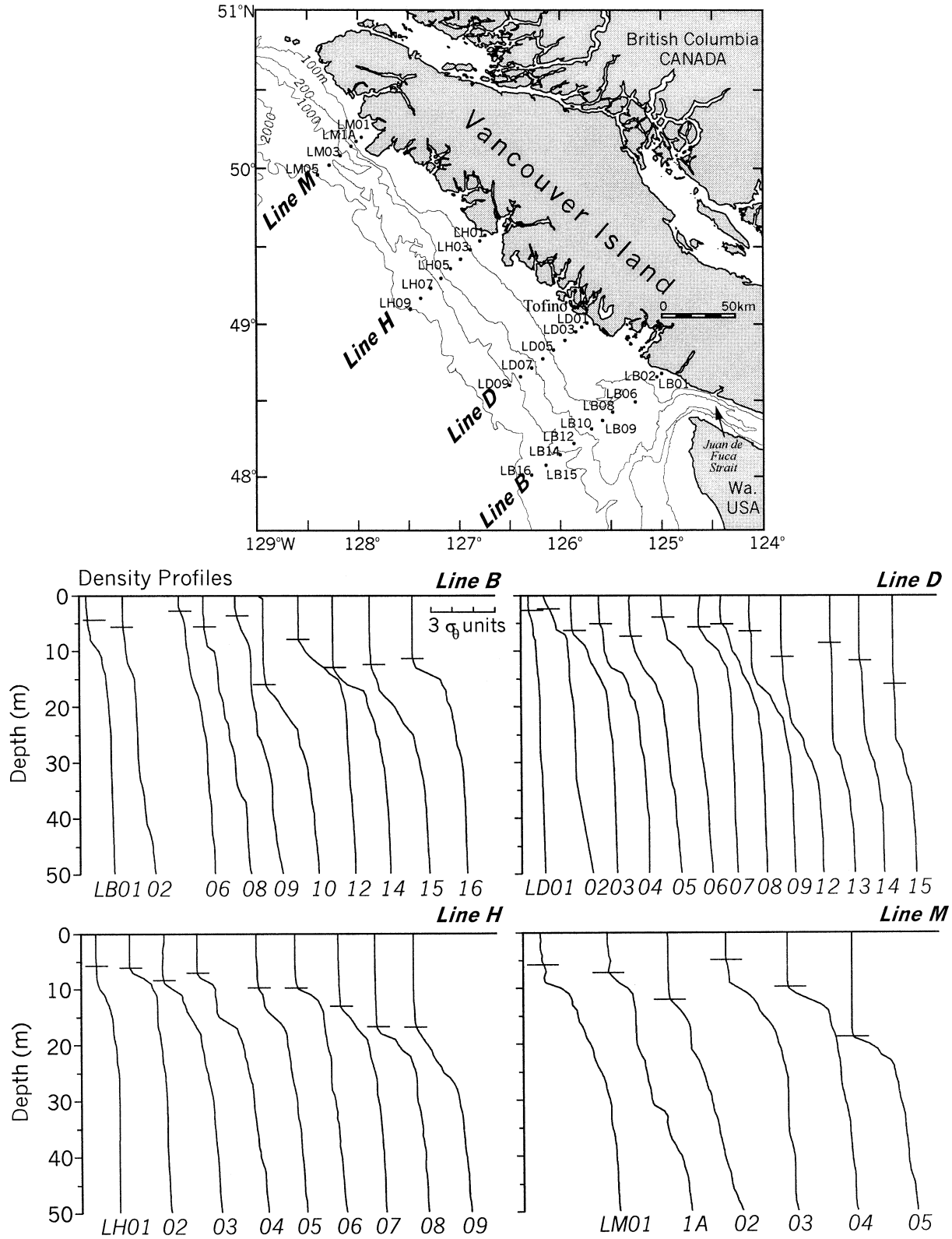

FIG. 3. Top portion of 1-m average density (σ_θ) profiles derived from CTD casts collected in Jul 1997 off the west coast of Vancouver Island (see map). Horizontal bars denote mixed layer depth derived using the SM algorithm. Profiles of σ_θ typically range from 22 to 25 kg m^{-3}. A scale of three σ_θ units is shown in the line B profile plots.

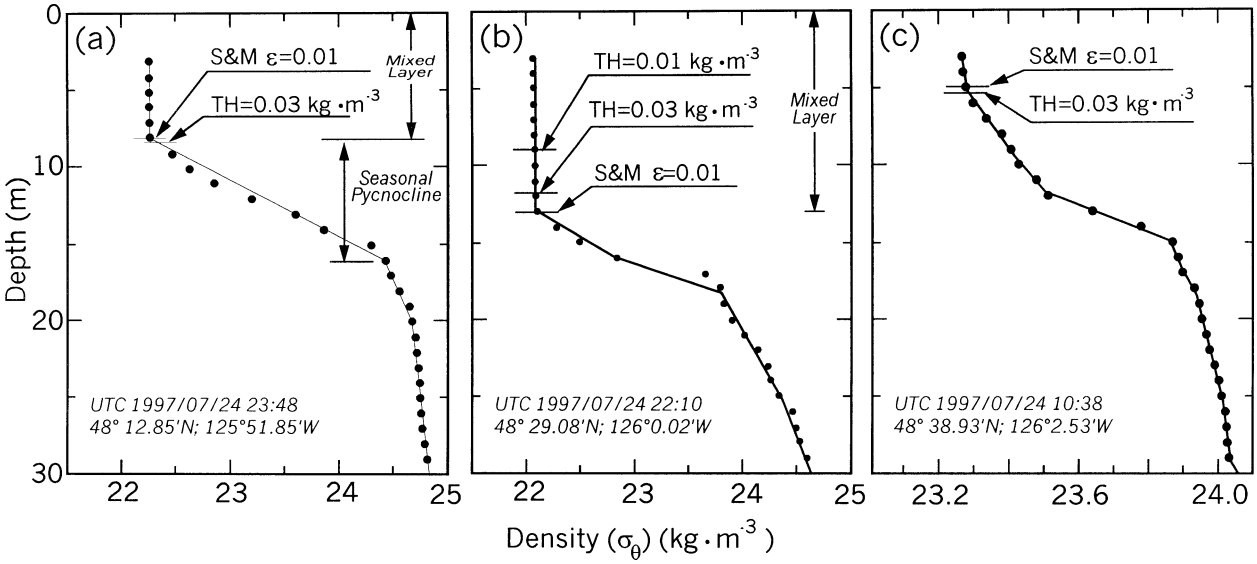

FIG. 4. The 1-m average density profile data (solid dots) and line segments fitted using the SM method for line B for 24 Jul 1997 (for location, see Fig. 3). Depth estimates for the SM method use $\varepsilon = 0.01$ and those for the threshold difference method (TH) use both $\Delta\sigma_\theta = 0.01$ and 0.03 kg m^{-3}. (a) A well-defined mixed layer, and underlying pycnocline; (b) less well-defined mixed layer and pycnocline; and (c) a poorly defined (essentially, nonexistent) mixed layer and pycnocline. Time and positional coordinates for each profile are shown. To avoid prop-wash and ship-wake contamination, the top 2.5 m of each profile has been omitted.

originates with internal wave motions, measurement limitations, and other factors—differs among the three methods. Our contention that the SM method ''outperforms'' the two threshold methods is based primarily on the smaller standard error for the SM method (Table 2a) and on the smaller percentage change in mixed layer depth caused by the incremental changes in the applied error norm relative to corresponding changes in the threshold levels (Fig. 5). Twenty-five estimates were used to construct each of the curves in Fig. 5, with values increasing from 0.004 kg m^{-3} in steps of 20% for the threshold difference method, from 0.0015 kg m^{-4} in steps of 15% for the threshold gradient method, and from 0.001 in steps of 20% for the SM method. As the thresholds and error norm are increased, estimates of the mean mixed layer depth increase (from roughly 10 to 20 m) and the standard error decreases. Assuming that true mixed layer depth variability due to internal waves and other factors contributes equally to the threshold and SM methods, we conclude that the threshold methods have greater variance than the SM method because of higher computational inaccuracy. For the error norm ranges considered, the SM method is a slightly better estimator.

4. Discussion and summary

The split-and-merge algorithm provides an accurate and flexible new method for estimating the depth of the surface mixed layer from oceanic profiles. The method eliminates the need for good initialization of the computation and allows for the ''fit'' of a variable number of linear segments to the profile data. Along with estimates of mixed layer depth, the method can be used to delineate other structural features of the upper ocean such as the gradient of the main pycnocline and the depth to the top of the thermocline (TTC).

Our intercomparison among the various depth estimators (the SM method, two threshold-type methods, the two- and three-step regression methods, and the integral-scale method) demonstrates that, in the absence of turbulent dissipation measurements, only the threshold and SM methods provide accurate estimates of mixed layer depth. This is clearly borne out by the mixed layer depth estimates obtained for two decades of density profiles collected off the west coast of Vancouver Island. According to results in Table 2a, the ~60 m mean depth obtained from the two-step regression and integral-scale methods (which is roughly five times the

TABLE 2a. The mean mixed layer depth (MLD_{sub}) and standard error (std dev divided by $\sqrt{N}$, N = number of samples) for different estimation methods. Subscripts SM, TH, and GR denote the SM, threshold difference, and threshold gradient methods, respectively; D_σ is the integral depth scale, D_2 is the MLD from the two-step function, and D_3 for the three-step function approach. The SM method uses an error norm $\epsilon = 0.003$.

	MLD_{SM}	MLD_{TH}	MLD_{GR}	D_σ	D_2	D_3
Mean (m)	(12.51 ± 0.32)	(12.43 ± 0.33)	(12.57 ± 0.38)	(60.4 ± 0.6)	(60.9 ± 0.7)	(35.60 ± 0.46)

TABLE 2b. The correlation-squared (r^2) matrix. (See Table 2a for terminology.)

	MLD_{SM}	MLD_{TH}	MLD_{GR}	D_σ	D_2	D_3
MLD_{SM}	1	0.90	0.76	0.28	0.09	0.11
MLD_{TH}	—	1	0.79	0.29	0.10	0.12
MLD_{GR}	—	—	1	0.30	0.10	0.13
D_σ	—	—	—	1	0.71	0.29
D_2	—	—	—	—	1	0.13

~12 m mean depth from the SM and threshold methods, and three times the ~35 m mean depth for the three-step regression method) is actually an estimate of the permanent pycnocline depth rather than the depth of the much shallower surface mixed layer. Similar results are obtained when the MLD data are analyzed according to season (Fig. 6). For the SM and threshold methods, the seasonal-mean MLD is shallower and associated confidence intervals more tightly constrained with depth for all seasons compared with the integral and regression methods. The normal MLD confidence distributions for the regression and integral methods are more reminiscent of random processes than natural variability associated with the spatial and temporal variations in MLD.

Of the two most accurate methods, the SM method yields a marginally lower standard error than the threshold difference method. This error arises from computational inaccuracy as well as from temporal and spatial variability in mixed layer depth arising from surface heating/cooling, internal wave displacements, and other physical processes. If we assume that smaller standard error is synonymous with improved computational skill, then the SM method slightly ''outperforms'' the threshold difference method in its ability to determine the surface mixed layer depth (the SM and threshold methods would yield the same variance in mixed layer depth if it were not for the slightly better computational accuracy of the SM method). In effect, the SM method provides an additional tool for estimating mixed layer depth from profile data. The greater computational complexity of the SM method is compensated for by its slightly greater reliability and its added ability to simultaneously determine additional structural features of the upper ocean.

Acknowledgments. We thank Alexander Rabinovich, Evgueni Kulikov, Ken Denman, and several anonymous reviewers for their valuable comments on the manuscript, and Patricia Kimber for her assistance with the figures.

APPENDIX

Steps in the SM Method

The problem of finding the ''best'' piecewise-linear approximation to the N-point curve $S = \{(z_i, \phi_i), i = 1, 2, \ldots, N\}$ generally proceeds in one of two ways:

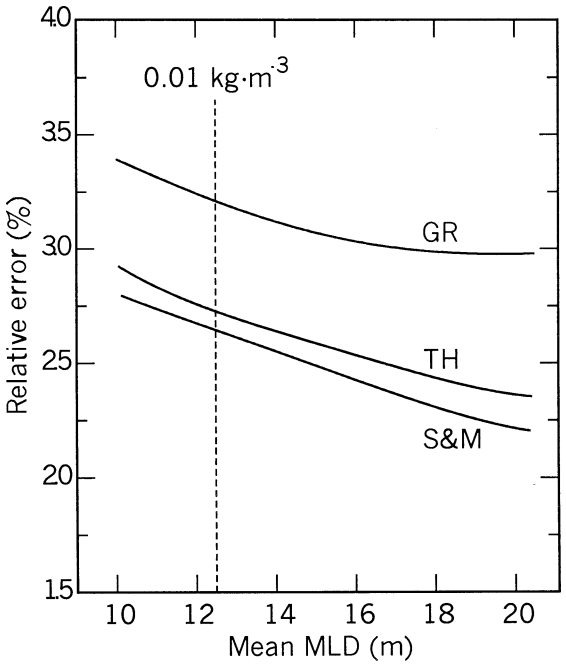

FIG. 5. Relative error (= std dev in depth estimate divided by $\sqrt{(N-1)}$) for N estimates calculated as the percentage of the mean mixed layer depth (summer-only data, west coast of Vancouver Island): GR = threshold gradient method; TH = threshold difference method; and SM = split-and-merge method. Each curve covers a broad range of 25 error norm (or threshold) values. The vertical line denotes the mean mixed layer depth for the de facto standard threshold difference, $\Delta\sigma_\theta = 0.01$ kg m^{-3}.

1) find the smallest number of subsets n such that the specified error norm, the statistical measure used to define the difference between the measured and fitted curves, does not exceed a given bound, or 2) minimize the error norm for a given n. Approach 1 usually involves a linear scan of the data points to be approximated and has a computational time of order $N \log N$ or N^2 (Ramer 1972). Approach 2 begins with small increments in the locations of the ''break points'' (subset boundaries where there are ''abrupt'' changes in slope) and, in the worst case, requires about N iterations. The worst case occurs when all the break points are clustered at the ''wrong'' end and have to be moved across the entire array of data points (Pavlidis and Horowitz 1974). For most other methods, initialization is critical, but is itself a nontrivial problem. The SM algorithm not only eliminates the need for ''good'' initialization but also allows for a variable number of segments. In effect, the method attacks the problem of approach 1 using the algorithms for approach 2, with a significant decrease in computing time.

The task is to determine the minimum number n such that the set of points S is divided into n subsets $S_1, S_2, \ldots, S_n$, where, for each subset, the data points are approximated by a linear polynomial of the form $\phi_k(z) = a_k + b_k z$, $k = 1, 2, \ldots, n$ with an error of less than some prescribed quantity ε and where the coefficients

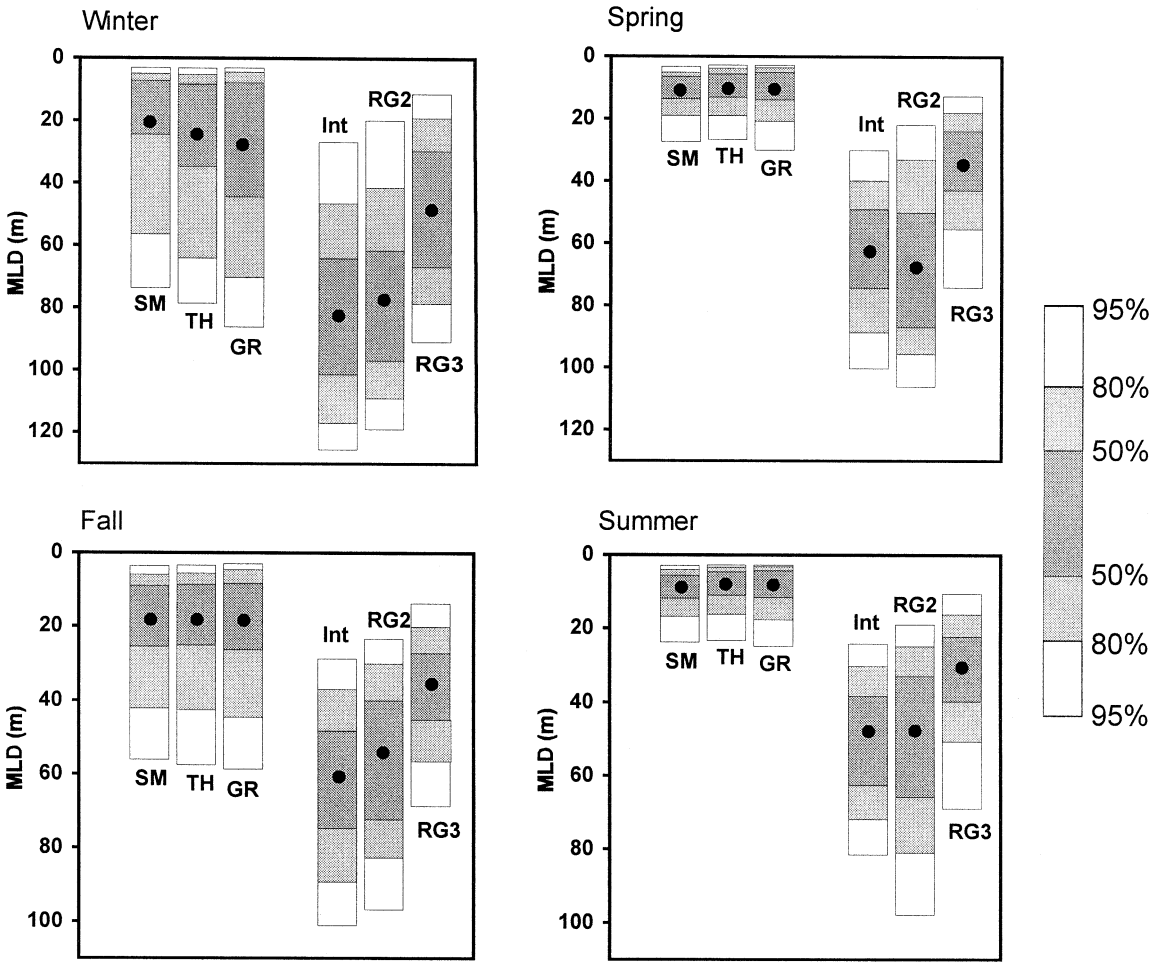

FIG. 6. Seasonal mean mixed layer depths (solid dots) and associated percentage confidence intervals based on CTD data for the west coast of Vancouver Island for the period 1978–2000. Winter = Jan–Feb–Mar, spring = Apr–May–June, summer = July–Aug–Sep, and fall = Oct–Nov–Dec. GR = threshold gradient method, TH = threshold difference method, SM = split-and-merge method, Int = integral method, RG2 = two-step regression, and RG3 = three-step regression.

a_k and b_k are found using the least squares method. For the first subset (here, the mixed layer), the constant $b_1 = 0$. The choice of the error norm ε, which defines how well the fitted curves match the observations, depends to some extent on the application and is commonly defined in two ways: 1) through the integral square error $\varepsilon_k^{(1)}$ where

$$\varepsilon_k^{(1)} = \sum_i \varepsilon_{ik}^2, \quad \text{for } (z_i, \phi_i) \in S_k,$$

and 2) by the maximum error $\varepsilon_k^{(2)}$ where

$$\varepsilon_k^{(2)} = \max(\varepsilon_{ik}), \quad \text{for } (z_i, \phi_i) \in S_k$$

and where $\varepsilon_{ik} = |\phi_i - \phi_k(z_i)|$. Sensitivity to noise is an important difference between the $\varepsilon_k^{(1)}$ and $\varepsilon_k^{(2)}$ norms.

Methods used to find the best piecewise-linear polynomial approximation to a curve almost always involve a linear scan of the points to be approximated, possibly with repetitions. The process of break-point adjustment can be accelerated substantially if one is allowed to split segments with large error norms and to merge adjacent segments with similar approximating coefficients (i.e., ''split and merge''). The fundamental steps in the spit-and-merge method are as follows:

Step 1 (the split procedure)—For an arbitrary initial subset $k = 1, 2, \ldots, n_r$, obtain the polynomial fit and check to see if the error norm ε_k for this fit exceeds the imposed limit, ε. (Here, we can use $n_r = 2$ since the program automatically adjusts to find the appropriate number of subsets for the specified error norm.) If $\varepsilon_k > \varepsilon$, split the kth subset into two parts and increment the number of subsets to $n_r + 1$. The dividing point of the kth subset is determined according to the following rule: If there are two or more points where the pointwise error is maximum, then use as a dividing point the midpoint between a pair of them. Otherwise, divide the segment S_k in half. Calculate the error norms ε_k on each new interval.

Step 2 (the merge procedure)—For $k = 1, 2, \ldots, n_r$, merge segments S_k and S_{k+1} provided that this will result in a new segment with $\varepsilon_k \leq \varepsilon$. Then, decrease n_r by unity to $n_r - 1$ and calculate the error norm on each new interval.

Step 3 (the break-point adjustment procedure)—For $k = 1, 2, \ldots, n_r - 1$, for every adjacent pair of subsets (S_k and S_{k+1}), scan the position of the break points to decrease the maximum of the error (ε_k, ε_{k+1}).

Step 4—If no changes in the segments have occurred in any of steps 1–3 above, then terminate. Or else go to step 1.

The above procedure is an algorithm that terminates after a local minimum *n*, for the number of segments is reached and the criterion for the termination is satisfied. The algorithm computational time is linear in *N*, even for the worst cases.

REFERENCES

Brainerd, K. E., and M. C. Gregg, 1995: Surface mixed and mixing layer depths. *Deep-Sea Res.*, **42A,** 1521–1543.

Curry, P., and C. Roy, 1989: Optimal environmental window and pelagic fish recruitment success in upwelling areas. *Can. J. Fish. Aquat. Sci.*, **46,** 670–680.

Denman, K. L., and A. E. Gargett, 1988: Multiple thermoclines are barriers to vertical exchange in the subarctic Pacific during SUPER, May 1984. *J. Mar. Res.*, **46,** 77–103.

Dodimead, A. J., F. Favorite, and T. Hirano, 1963: Salmon of the North Pacific Ocean. Part II: Review of oceanography of the subarctic Pacific region. International North Pacific Fisheries Commission, Bull. 13, Vancouver, BC, Canada, 195 pp.

Freeland, H., K. Denman, C. S. Wong, F. Whitney, and R. Jacques, 1997: Evidence of change in the winter mixed layer in the northeast Pacific Ocean. *Deep-Sea Res.*, **44A,** 2117–2129.

Garwood, R. W., 1977: An oceanic mixed layer model capable of simulating cyclic states. *J. Phys. Oceanogr.*, **7,** 455–471.

Kantha, L. H., and C. A. Clayson, 1994: An improved mixed layer model for geophysical applications. *J. Geophys. Res.*, **99,** 25 235–25 266.

Kara, A. B., P. A. Rochford, and H. E. Hurlburt, 2000a: An optimal definition for ocean mixed layer depth. *J. Geophys. Res.*, **105,** 16 803–16 821.

——, ——, and ——, 2000b: Mixed layer depth variability and barrier layer formation over the North Pacific Ocean. *J. Geophys. Res.*, **105,** 16 783–16 801.

Large, W. G., J. C. McWilliams, and S. C. Doney, 1994: Oceanic vertical mixing: A review and a model with nonlocal boundary layer parameterization. *Rev. Geophys.*, **32,** 363–403.

Levitus, S., 1982: *Climatological Atlas of the World Ocean.* NOAA Prof. Paper 13, 173 pp. and 17 microfiche.

Lukas, R., and E. Lindstrom, 1991: The mixed layer of the western equatorial Pacific Ocean. *J. Geophys. Res.*, **96,** 3343–3358.

Martin, P. J., 1985: Simulation of the mixed layer at OWS November and Papa with several models. *J. Geophys. Res.*, **90,** 903–916.

Papadakis, J. E., 1981: Determination of the wind mixed layer by an extension of Newton's method. Pacific Marine Sci. Rep. 81-9, Institute of Ocean Sciences, Sidney, BC, Canada, 32 pp.

——, 1985: On a class of form oscillators. *Speculations Sci. Technol.*, **8,** 291–303.

Pavlidis, T., and S. L. Horowitz, 1974: Segmentation of plan curves. *IEEE Trans. Comput.*, **C-23,** 860–870.

Peters, H., M. C. Gregg, and J. M. Toole, 1988: On the parameterization of equatorial turbulence. *J. Geophys. Res.*, **93,** 1199–1218.

——, ——, and ——, 1989: Meridional variability of turbulence through the equatorial undercurrent. *J. Geophys. Res.*, **94,** 18 003–18 009.

Price, J. F., R. A. Weller, and R. Pinkel, 1986: Diurnal cycling: Observations and models of the upper ocean response to diurnal heating, cooling, and wind mixing. *J. Geophys. Res.*, **91,** 8411–8427.

Ramer, U., 1972: An iterative procedure for the polygonal approximation of plane curves. *J. Comput. Graphics Image Process.*, **1,** 244–256.

Robinson, C. L. K., and D. M. Ware, 1994: Modeling pelagic fish and plankton trophodynamics off southwestern Vancouver Island, British Columbia. *Can. J. Fish. Aquat. Sci.*, **51,** 1737–1751.

——, ——, and T. R. Parsons, 1993: Simulated annual plankton production in the northeastern Pacific coastal upwelling domain. *J. Plankton Res.*, **15** (2), 161–183.

Schneider, N., and P. Müller, 1990: The meridional and seasonal structures of the mixed-layer depth and its diurnal amplitude observed during the Hawaii-to-Tahiti Shuttle experiment. *J. Phys. Oceanogr.*, **20,** 1395–1404.

Skyllingstad, E. D., W. D. Smyth, J. N. Moum, and H. Wijesekera, 1999: Upper-ocean turbulence during a westerly wind burst: A comparison of large-eddy simulation results and microstructure measurements. *J. Phys. Oceanogr.*, **29,** 5–28.

Smyth, W. D., D. Hebert, and J. N. Moum, 1996a: Local ocean response to a multiphase westerly windburst. Part 1: The dynamic response. *J. Geophys. Res.*, **101,** 22 495–22 512.

——, ——, and ——, 1996b: Local ocean response to a multiphase westerly windburst. Part 2: Thermal and freshwater responses. *J. Geophys. Res.*, **101,** 22 513–22 533.

Sprintall, J., and D. Roemmich, 1999: Characterizing the structure of the surface layer in the Pacific Ocean. *J. Geophys. Res.*, **104,** 23 297–23 311.

Washburn, L., B. M. Emery, B. H. Jones, and D. G. Ondercin, 1998: Eddy stirring and phytoplankton patchiness in the subarctic North Atlantic in late summer. *Deep-Sea Res.*, **45A,** 1411–1439.

Weller, R. A., and A. J. Plueddemann, 1996: Observations of the vertical structure of the oceanic boundary layer. *J. Geophys. Res.*, **101,** 8789–8806.

Wijesekera, R. W., and M. C. Gregg, 1996: Surface layer response to weak winds, westerly bursts, and rain squalls in the western Pacific warm pool. *J. Geophys. Res.*, **101,** 977–997.

Wijffels, S., E. Firing, and H. Bryden, 1994: Direct observations of the Ekman balance at 10°N in the Pacific. *J. Phys. Oceanogr.*, **24,** 1666–1679.